Crystal structure of a T cell receptor bound to an allogeneic MHC molecule

Jean-Baptiste Reiser[1], Claudine Darnault[1], Annick Guimezanes[2], Claude Grégoire[2], Thomas Mosser[2], Anne-Marie Schmitt-Verhulst[2], Juan Carlos Fontecilla-Camps[1], Bernard Malissen[2], Dominique Housset[1] and Gilbert Mazza[2]

Many T cell receptors (TCRs) that are selected to respond to foreign peptide antigens bound to self major histocompatibility complex (MHC) molecules are also reactive with allelic variants of self-MHC molecules. This property, termed alloreactivity, causes graft rejection and graft-*versus*-host disease. The structural features of alloreactivity have yet to be defined. We now present a basis for this cross-reactivity, elucidated by the crystal structure of a complex involving the BM3.3 TCR and a naturally processed octapeptide bound to the H-2K^b allogeneic MHC class I molecule. A distinguishing feature of this complex is that the eleven-residue-long complementarity-determining region 3 (CDR3) found in the BM3.3 TCRα chain folds away from the peptide binding groove and makes no contact with the bound peptide, the latter being exclusively contacted by the BM3.3 CDR3β. Our results formally establish that peptide-specific, alloreactive TCRs interact with allo-MHC in a register similar to the one they use to contact self-MHC molecules.

The specificity of T cell recognition is determined by the variable (V) domain of the T cell receptor (TCR) α and β chains[1]. TCR-peptide–MHC (pMHC) class I complexes for which crystal structures have been determined (mouse[2], 2C–dEV8–H-2K^b, human[3,4]: A6–Tax–HLA-A2 and B7–Tax–HLA-A2) indicate a common diagonal docking mode that maximizes contact of the TCR with the pMHC surface. To evaluate the generality of these findings and determine whether they extend to allorecognition, we have focused our efforts on solving the crystal structure of a mouse TCR in complex with an allogeneic MHC molecule. MHC alleles can differ from one another by up to 20 amino acids and most of these polymorphic residues line the peptide-binding cleft and determine peptide-binding specificity. Nevertheless, the few polymorphic residues that are exposed on the outer surface of the MHC α-helices and available for TCR contact could lead alloreactive TCR to adopt an MHC-binding register distinct from the one used to contact the self-MHC molecules with which they have been selected to cooperate. Along that line, it has been suggested that alloreactive T cells mainly focus on the polymorphic residues contributed by the MHC α-helices and act in a peptide-independent mode. In contrast to the latter hypothesis, our results underline the similarity between allorecognition and the recognition of foreign peptides bound to self-MHC molecules. Our data also indicate that peptide-specific alloreactive TCRs contact the allo-MHC surface through a geometry similar to the one the TCR initially uses to contact the self-MHC molecules responsible for their selection.

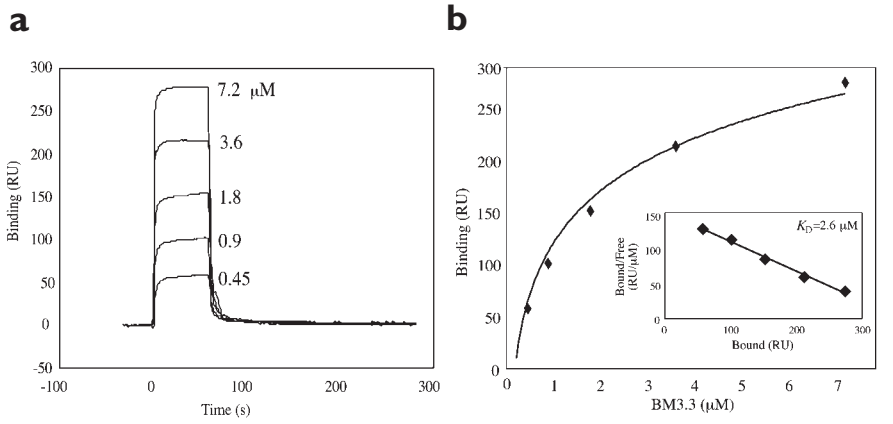

Figure 1. The affinity of BM3.3 scFv TCR binding to the pBM1–H-2K^b alloantigen. (**a**) Surface plasmon resonance demonstrates BM3.3 TCR binding to pBM1–H-2K^b complexes. Following purification, BM3.3 scFv TCR was injected at the indicated concentrations and at a flow rate of 5 μl/min over surfaces to which relevant (pBM1–H-2K^b, 2167RU) or irrelevant (pKB3–H-2K^b, 2286 RU) pMHC class I complexes had been immobilized. The traces shown have had their corresponding background responses (obtained following injection over the pKB3–H-2K^b surface) substracted. (**b**) The difference between the responses at equilibrium in the pBM1–H-2K^b and pKB3–H-2K^b flow cells is plotted for each BM3.3 scFv TCR concentration. Inset: Scatchard transformation of the data. The K_D value of 2.6 μM was obtained from the slope by linear regression. One representative experiment of three is shown.

[1]Laboratoire de Cristallographie et Cristallogénèse des Protéines, Institut de Biologie Structurale J.-P. Ebel, CEA-CNRS-UJF, 41, rue Jules Horowitz, F-38027 Grenoble Cedex 1, France. [2]Centre d'Immunologie INSERM-CNRS de Marseille-Luminy, Case 906, F-13288 Marseille Cedex 9, France. Correspondence should be addressed to D. H. (housset@lccp.ibs.fr).

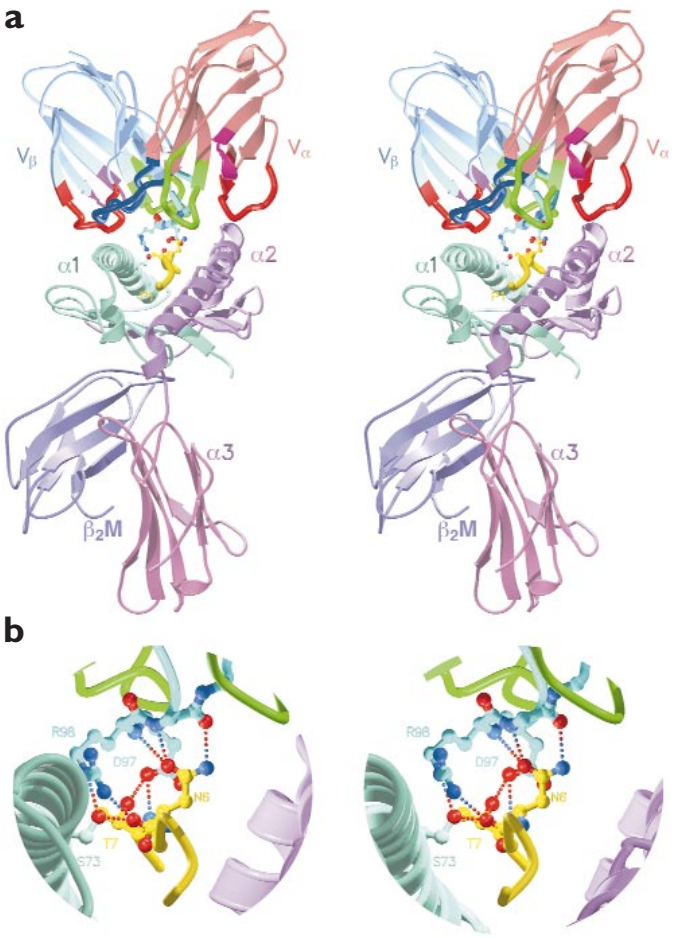

Figure 2. Structure of the BM3.3–pBM1–H-2K^b complex. (**a**) Stereoscopic view showing the overall orientation of the BM3.3 scFv TCR to pBM1–H-2K^b. The TCR is on top and the peptide N-terminus is oriented towards the viewer. The β-strands of each component are represented as arrows. Domains are color-coded as follows: TCR V_α (light red), TCR V_β (light blue), H-2K^b α1 domain (green), H-2K^b α2 domain (light purple), H-2K^b α3 domain (pink), β_2-microglobulin (dark purple). The peptide is depicted as a yellow tube; side chains involved in TCR interaction are shown in ball-and-stick format. The CDR1 and CDR2 loops from V domains are drawn as green and red thick tubes, respectively. CDR3α is depicted in dark blue and CDR3β in cyan. This view also highlights that the V_β2 domain used by the BM3.3 TCR has its c″ β-strand switched to the outer β-sheet and thus resembles V_α domains in terms of its secondary structure. Therefore, determination of the V_β2 structure as the antigen component of an antigen-antibody complex[32], or as part of a TCR-pMHC complex (this paper), shows that the c″ β-strand switch constitutes a genuine structural feature of this V_β domain (an r.m.s. difference of 0.5 Å is obtained for the position of 95 pairs of α-carbons corresponding to residues 1 to 95) that distinguishes it from all the other V_β domains analyzed to date. (**b**) Close-up view of the TCR-pMHC interface showing CDR3β blanketing the C-terminus of the peptide. Direct hydrogen bonds between the TCR and the peptide are shown as dotted lines. The TCR-pMHC complex is oriented as in **a**. Also shown is Ser[73] of the H-2K^b α1-helix, a residue expected to play a critical role in allorecognition of H-2K^b by the BM3.3 TCR.

Results

Overview of the complex structure

The structure of the BM3.3 cytotoxic TCR in complex with a naturally processed octapeptide (pBM1: INFDFNTI) bound to the H-2K^b allogeneic MHC class I molecule has been determined by molecular replacement and refined to 2.5 Å resolution (see Methods). Using surface plasmon resonance, the BM3.3 TCR was found to bind pBM1–H-2K^b complexes with a K_D of 2.6 μM at 25 °C (**Fig. 1a,b**), a value at the higher end of the range reported for TCR-pMHC interactions[5]. The BM3.3 TCR assumes a diagonal orientation relative to the long axis of the peptide-binding groove that is similar to that of TCRs bound to self-MHC class I molecules (**Fig. 2a**). The total surface area buried in the BM3.3–pBM1–H-2K^b interface (1478 Å^2) is the smallest of the TCR-pMHC complexes of known structure (see Web Table 1 on the supplementary information page of *Nature Immunology* online) and the V_α domain contributes only 38% of the BM3.3 TCR buried surface area. This contrasts with the other complexes in which V_α contribution is equivalent (2C) or almost twice as great (A6 and B7) as that of the V_β domain. Two reasons account for this limited V_α contribution. First, the 11-residue-long CDR3α bends away from the peptide-binding groove (**Fig. 2a,b**) and contacts a single residue of the pMHC surface (Gln[65] of the MHC α1-helix), contributing the least buried surface of the six complementarity-determining regions (CDRs). Second, due to the unusual orientation of both CDR3α and the 9-residue-long CDR3β (see below), CDR1α and CDR2α are shifted towards the amino-terminus of the MHC α2-helix and away from the pMHC surface, thereby limiting their interaction with the MHC α-helices. Therefore, the presence of a long CDR3α within a TCR neither prevents ligand recognition in an MHC-restricted way[6] nor does it necessarily raise its peptide specificity. At odds with previous conclusions[2–4], this new structure also shows that a V_β domain can dominate TCR-pMHC class I interaction and that CDR3α is not always a site of contact with peptide side chains.

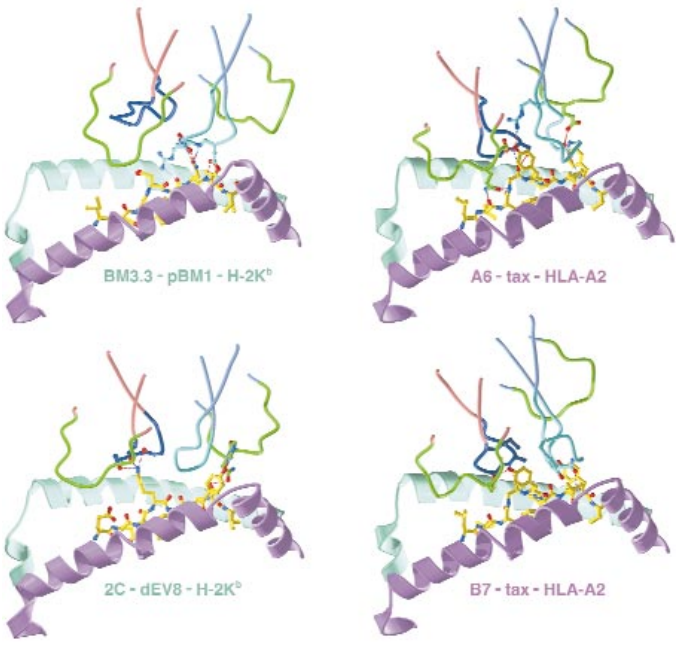

Figure 3. Peptide-TCR interactions occurring at the interface of four TCR-pMHC class I complexes. In this representation, the TCR-pMHC complex is viewed from the side so that the MHC α2-helix (light purple) is in the foreground and the MHC α1-helix (green) is behind the peptide (yellow). CDR2s have been removed for clarity. CDR1 and CDR3 are shown as a backbone worm diagram and color-coded as follows: CDR1α and β (green), CDR3α (dark blue), CDR3β (cyan). The peptide residues involved in contact with the TCR are shown in ball-and-stick format. The corresponding hydrogen bonds are drawn as dotted lines. This representation highlights the different bends adopted by the tip of the CDR3β loop according to the length and conformation of the MHC-bound peptide.

Antigenic peptide recognition

Although the conformation of the bound pBM1 peptide is similar to that of the dEV8 peptide found in the 2C–dEV8–H-2K^b complex (r.m.s. difference of 0.47 Å), their respective "read-out" by the corresponding TCRs differs substantially. In the BM3.3–pBM1–H-2K^b complex, it is entirely mediated by the CDR3β, whereas in the 2C–dEV8–H-2K^b complex, it relies on residues that belong to both the V_α and V_β domains (**Fig. 3**). Consistent with functional studies using alanine-substituted pBM1 peptide variants, direct TCR interactions are restricted to residues Asn^6 and Thr^7 of the pBM1 peptide (**Fig. 4**), whereas in the case of dEV8, an additional Lys at position P4 establishes several direct contacts with CDR3α (**Tables 1** and **2**). There seems to be sufficient space between the pBM1 peptide and BM3.3 TCR to accommodate several different amino acid replacements at positions P1 and P4: even in the case of an aspartic acid to lysine substitution at position P4 of pBM1, the distal tip of the extended lysine side chain will still be too short to interact directly with the BM3.3 CDR3α. Consequently, this should increase the theoretical number of K^b-presentable octapeptides with which BM3.3 could successfully interact by approximately 400 times. Consistent with this expected peptide permissiveness, the BM3.3 TCR fortuitously recognized one (VSV8: RGYVYQGL) out of three octapeptides selected for their ability to bind to H-2K^b (ref. 7). Comparison of the outward-facing side chains found in pBM1 and VSV8 shows a conservative replacement (asparagine to glutamine) at the primary TCR contact residue found at position P6. Therefore, two minimally homologous peptides can productively interact with the same alloreactive TCR as long as they possess both a proper set of MHC binding sites and a related amino acid at one primary T cell contact position[8].

The exclusive role played by the BM3.3 CDR3β in peptide recognition is consistent with the fact that its apex folds back towards the peptide NH_2-terminus and occupies the center of the contact interface (**Fig. 2b**). This differs from the conformation of the A6 and B7 CDR3βs that fold back towards the peptide carboxy-terminus, thereby contributing to the formation of a deep pocket that accommodates the up-facing tyrosine side chain at position P5 of the Tax peptide (**Fig. 3**). A similar central pocket present in the 2C TCR binding site likely accounts for its ability to accommodate the pronounced bulge found at the COOH-terminus of H-2L^d–bound peptides[9]. Thus, the CDR3β conformation found in BM3.3, and plausibly in N15[10], TCRs seems adapted to maximize the 'read-out' of the COOH-terminal residues of peptides that bind, in an extended or slightly arched conformation, deep in the H-2K^b–binding cleft. On the other hand, the CDR3β conformation found in A6 and B7 seems better suited to recognize peptides that, due to their length or to their binding to much shallower MHC clefts, have more substantial bulges in their centers or at their COOH-termini[11].

Water molecules in the buried surface

The BM3.3–pBM1–H-2K^b structure is the first in which a significant number of water molecules are involved in the TCR-pMHC interface. (In the 2C–dEV8–H-2K^b complex[2],

Table 1. Comparison of the TCR-pMHC interactions in TCR-pMHC class I complexes of mouse origins for which crystal structures have been determined

BM3.3–pBM1–H-2K^b (PDB entry: 1FO0)			**2C–dEV8–H-2K^b*** (PDB entry: 2CKB)		
BM3.3	**PBM1**		**2C**	**dEV8**	
Hydrogen bonds**			Hydrogen bonds		
D97β OD1	N T7		S93α O	NZ K4	
D97β OD1	OG1 T7		G99α O	NZ K4	
R98β N	OD1 N6		N30β N	OH Y6	
R98β NH2	O F5		N30β OD1	OH Y6	
V99β N	OD1 N6		*N30β ND2*	*OG S7*	
V99β O	ND2 N6		*Y50β O*	*OG S7*	
W31β NE1	Wat	OG1 T7	Y31α OH	Wat	OE1 E1
R50β NH1					
R98β NH2	Wat	OD2 D4			
VDW contacts**		No. of cont	VDW contacts		No. of cont
D97β	N6, T7	6, 2	A101α	K4	5
V99β	D4, N6	2, 3	N30β	Y6, S7	3, 2
			G96β	Y6	2
BM3.3	**H-2K^b**		**2C**	**H-2K^b**	
Hydrogen bonds			Hydrogen bonds		
Q27α NE2	OE2 E58		*S27α N*	*OE2 E58*	
Q27α OE1	NH2 R62		S27α O	NH1 R62	
S29α OG	OG1 T163		S27α OG	OE1 E58	
K53α NZ	OE1 E154		S27α OG	OE2 E58	
G98α N	OE1 Q65		Y31α OH	NE R155	
S51β OG	NH2 R79		K68α NZ	OE1 E166	
S51β OG	NH1 R79		*N28β ND2*	*NZ K146*	
D97β OD2	NZ K146		A52β O	NH1 R79	
R98β NE	O G69				
R98β NE	OG S73				
R98β NH2	OG S73				
R98β NH2	OD1 N70				
VDW contacts		No. of cont	VDW contacts		No. of cont
Q27α	R62	2	Y26α	R62	7
F31α	R155	2	S27α	E58	2
Y52α	E154	6	A28α	R62	2
	R155	6	Y31α	R155	6
	A158	4	Y50α	R155	14
K53α	E154	3		A158	2
W31β	V76	2	S51α	A158	2
R50β	V76	3	F100α	R62	4
D97β	K146	2		Q65	10
R98β	G69	2	N28β	K146	2
V99β	R155	3	H29β	A150	2
			Y50β	V76	2
			G97β	R155	3

TCR-peptide contacts are shown in the upper section and TCR-MHC contacts are listed in the bottom section. Only those TCR with at least two van der Waals (VDW) contacts with the pMHC surface have been included. The water molecules that form hydrogen bond bridges between the TCR and the MHC (10 in the BM3.3–pBM1–H2-K^b, and 1 in the 2C–dEV8–H-2K^b complexes) are not listed. PDB, Protein Data Bank; No. of cont, number of contacts. *For the 2C–dEV8–H-2K^b structure, italicized characters denote interactions present in only one of the two TCR-pMHC complexes found in the asymmetric unit. **Distance cutoffs used in the Table are 3.65 Å for hydrogen bonds and 4.5 Å for van der Waals contacts.

Table 2. Comparison of the TCR-pMHC interactions in TCR-pMHC class I complexes of human origins for which crystal structures have been determined

A6–Tax–HLA-A2 (PDB entry: 1AO7)			**B7–Tax–HLA-A2** (PDB entry: 1BD2)		
A6	**Tax**		**B7**	**Tax**	
Hydrogen bonds			Hydrogen bonds		
Q30α OE1	N G4		D30α OD1	OH Y5	
Q30α NE2	O L2		G95α O	OH Y5	
S31α OG	OH Y5		A96α N	O G4	
T93α OG1	OH Y5		G98β O	N Y8	
S100α N	O G4				
S100α OG	O G4				
E30β OE1	OH Y8				
R95β NH2	OH Y5				
L98β O	N Y8				
VDW contacts	No. of cont		VDW contacts	No. of cont	
D99α	G4,Y5	4, 5	M28α	L1	4
S100α	Y5	6	D30α	Y5	2
L98β	Y8	8	Y31α	Y5	4
G100β	V7	3	M93α	Y5	3
P103β	Y5	6	G95α	G4,Y5	2, 5
			A96α	Y5	6
			Y96β	Y8	4
			G98β	V7,Y8	6,7
			G99β	V7	2
			Y104β	Y5	15
A6	**HLA-A2**		**B7**	**HLA-A2**	
Hydrogen bonds			Hydrogen bonds		
K1α N	OE2 E58		S27α O	NE1 W167	
Q30α NE2	NZ K66		S51α OG	O A158	
N52α ND2	OE2 E166		E94α O	NH1 R65	
K68α NZ	OG1 T163		E94α O	NH2 R65	
K68α NZ	OE1 E166		E94α OE1	NH2 R65	
T98α OG1	NH2 R65				
D99α OD1	NE R65				
D99α OD1	NH2 R65				
E101β N	O A150				
E101β O	NE2 Q155				
R102β NH1	O A149				
VDW contacts	No. of cont		VDW contacts	No. of cont	
D26α	E58	3	S27α	W167	3
R27α	W167	6	M28α	Y59	3
Y50α	A158	2		W167	5
K68α	E166	2	I52α	R157	2
D99α	R65	2		A158	9
D99α	K66	4		E161	2
W101α	R65	2	Q102α	R65	1
	K68	2		A69	1
	A69	8	K103α	R65	3
	Q72	4	Y48β	R65	2
G102α	R62	2			
L28β	Q72	2			
	T73	2			
R102β	A150	5			
P103β	Q155	2			

only three water-mediated hydrogen bonds have been reported: between $Tyr^{31\alpha}$ and Glu^{P1}, $Tyr^{31\alpha}$ and Glu^{P2}, and $Thr^{26\beta}$ and Glu^{149HC}.) Among the 12 water molecules that form hydrogen bond bridges between the BM3.3 TCR and the pMHC, two of them allow indirect contacts between the TCR and positions P4 and P7 of the peptide. Due to the unusual CDR3α loop conformation, a large cavity is found at the V_α-pMHC interface and filled with about 30 water molecules. Despite their refinement at resolutions similar to that of the BM3.3–pBM1–H-2K^b complex, well ordered water molecules contributing hydrogen bonds have not been reported for the A6–Tax–HLA-A2 and B7–Tax–HLA-A2 complexes[3,4]. In contrast, a network of well ordered water molecules is present at antibody-antigen interfaces and improves both their complementarity and their stability[12]. According to alanine-scanning mutagenesis (**Fig. 4**), the water-mediated contact involving the peptide P4 side chain does not measurably influence the peptide specificity of the BM3.3 TCR. Although the free energy contribution of water-mediated hydrogen bonds is significantly weaker than that of direct hydrogen bonds, it remains possible that, when considered collectively, the numerous water molecules bound in the BM3.3–pBM1–H-2K^b interface influence the specificity of the BM3.3 TCR.

Differences in two TCR-pMHC interfaces

Comparison of the BM3.3–pBM1–H-2K^b and 2C–dEV8–H-2K^b complexes allows us to determine whether common features exist when two distinct TCRs bind to the same MHC allele. The overall footprint of the BM3.3 TCR (**Fig. 5a**) is shifted towards the COOH-terminus of the bound peptide and twisted counterclockwise relative to the 2C TCR footprint (**Fig. 5b**). The same 17 MHC residues are partially or totally buried by both BM3.3 (out of 19 buried) and 2C (out of 22 buried) TCRs. However, the detailed interactions at the interface of the two TCRs and H-2K^b differ substantially. The 2C–H-2K^b interface is mainly hydrophobic, whereas polar interactions dominate the BM3.3–H-2K^b interface (**Table 1**). In both interfaces, only two MHC residues (Glu^{58} and Arg^{62}) form conserved hydrogen bonds with an identical TCR position (27α), although this position is occupied by different residues in the BM3.3 (glutamine) and 2C (serine) TCRs and assumes distinct spatial positions (the α-carbons are separated by more than 6 Å when the α1α2 domains of the H-2K^b molecules are superimposed). The network of van der Waals contacts differs as well and its most conserved element corresponds to a hydrophobic interaction between a tyrosine residue of CDR2α ($Tyr^{50\alpha}$ in 2C and $Tyr^{52\alpha}$ in BM3.3) and residues Arg^{155} and Ala^{158} of the MHC α2-helix (**Table 1**). Therefore, the number of conserved features existing in the contacts between BM3.3–H-2K^b and 2C–H-2K^b is even more limited than the few noted from the comparison of the A6–HLA-A2 and B7–HLA-A2 complexes[4].

Discussion

Before intrathymic TCRαβ selection, 5 to 20% of thymocytes can recognize the small set of self-MHC alleles expressed in any one individual[13,14], indicating that unselected TCRs have an intrinsic predisposition for interacting with MHC. From a structural standpoint, the concerted evolution of the V_α locus and of polymorphic MHC molecules might have shaped the

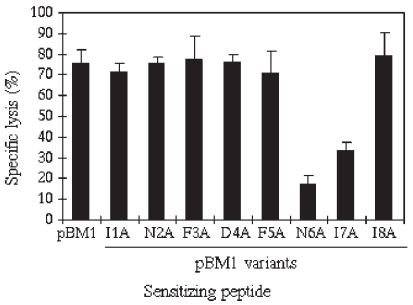

Figure 4. Identification of pBM1 amino acids critical for BM3.3 transgenic TCR recognition. Ala-substituted analogs of the pBM1 peptide show that position 6 and, to a lesser extent, position 7 are the most critical for recognition by T cells expressing the BM3.3 transgenic TCR. Data correspond to the percentage of specific lysis (mean ± s.d.) observed in three independent experiments done at an effector to target ratio of 5:1, and using RMA-S target cells pulsed with a 10^{-7} M concentration of peptide. Positions 6 and 7 are exposed to the solvent. Their substitution with alanine does not reduce the binding of the corresponding variant peptides to H-2K^b but does impair BM3.3 TCR recognition.

germline-encoded V_α gene segments so that conserved CDR1α and CDR2α residues interact with a conserved area of the MHC α-helices and help align the CDR3s on the most exposed section of the bound peptide. Due to their lack of involvement in some TCR-MHC class I complexes (**Tables 1** and **2**), CDR1β and CDR2β are unlikely to encode a plausible landmark. Comparison of the A6, B7 and 2C TCRs in complex with their pMHC ligands underscored that in each instance, Ser^{51} of CDR2α contacts Ala^{158} of the MHC α2-helix[2-4]. However, this single shared TCR-MHC contact, which may have constituted a pivot fixing the overall geometry of most TCR-pMHC class I interactions, is absent in the BM3.3–pBM1–H-2K^b complex (in the latter, Ser$^{51\alpha}$ makes no contact with the MHC; instead, the contiguous Tyr$^{52\alpha}$ contacts Ala^{158} of the MHC α2-helix). Therefore, although the tips of CDR1α and CDR2α footprint on a few turns of the MHC α2-helix that are rather conserved within MHC class I alleles (**Fig. 5c**), the detailed features of these interactions are very different (**Tables 1** and **2**). The present day V_α gene segments have evolved through several rounds of gene duplication[15]. In that process, the position and nature of the primordial set of CDR1 and CDR2 residues involved in recognizing a common MHC site and in steering the TCR orientation may have been blurred by subsequent drifting. As a result, the present day CDR1α-CDR2α combinations may each adopt a unique solution to binding to a given MHC surface. Considering that residues found at position 155 of the MHC α2-helix are prone to peptide-dependent conformational changes[16] and are sensed by the CDR2α loop of some TCRs (**Table 1**), the footprints of the same CDR1α-CDR2α combination docked onto the same MHC allele can still show slight differences depending on the nature of the bound peptide.

Figure 5. Docking of TCRs to pMHC class I ligands. All three stereoviews are looking directly onto the surface of the peptide–H-2K^b complex; in each, the C-terminus of the peptide is at the top. In (**a**) and (**b**), stereoviews represent the footprint of the molecular surface of the BM3.3 and 2C TCR binding sites on the peptide H-2K^b solvent-accessible surface, respectively. The H-2K^b surface is color-coded according to the CDRs that contact it: CDR1-buried (green), CDR2-buried (red), CDR3α-buried (blue) and CDR3β-buried (cyan). The CDRs are represented as thin worms using the same color code. The peptide backbone (thick worm) and its solvent-accessible surface are depicted in yellow. The H-2K^b α-helices are visible through the semitransparent surface and colored in light emerald green (α1) or light purple (α2). In the stereoview shown in (**c**), the α1/α2-helices of the MHC component found in various TCR-pMHC class I complexes were superimposed to highlight the differences occurring between the respective CDR footprints on pMHC class I ligands. The MHC α-helices and the CDRs have been drawn using the same color code as in **a** and **b**. The CDRs of the different TCRs are coded as follows: BM3.3 (thicker worm and fully saturated colors), 2C (dark colors), A6 (medium intensity colors) and B7 (pale colors).

Our results provide a structural glimpse at the molecular basis of alloreactivity, the ability for self-MHC–restricted TCRs to crossreact with allelic variants of self-MHC molecules[17]. Two models have been put forward to account for the observation that the frequency of alloreactive T cells specific for any given allogeneic MHC molecule is several orders of magnitude higher than that of T cells specific for any foreign peptide bound to self-MHC molecules. On the one hand, it has been proposed that alloreactive T cells recognize polymorphic determinants that are entirely contributed by the α-helices of the allogeneic MHC molecule[18]. This blindness *vis-à-vis* the bound peptide should give rise to an unusually high density of antigenic determinants per target cells and permit the activation of T cell clones of much lower affinity than those involved in peptide-dependent self-MHC–restricted responses. On the other hand, alloreactive T cell clones have been hypothesized to recognize allogeneic MHC molecules in a peptide-specific fashion[19]. Along this line, the high precursor frequency of alloreactive T cells is accounted for by the fact that allogeneic MHC molecules display a totally new constellation of endogeneous peptides to which the repertoire of mature T cells has not been negatively selected in the thymus. The structure of the BM3.3–pBM1–H-2K^b complex clearly supports the latter hypothesis in that it demonstrates that peptide residues constitute an integral component of the composite epitope recognized by the BM3.3 TCR on the allo-pMHC surface.

In a given individual, T cells are likely to adopt the same MHC-binding register during their selection in the thymus and once they act in the periphery. Considering the similarity between allorecognition and the recognition of foreign peptides bound to self-MHC molecules

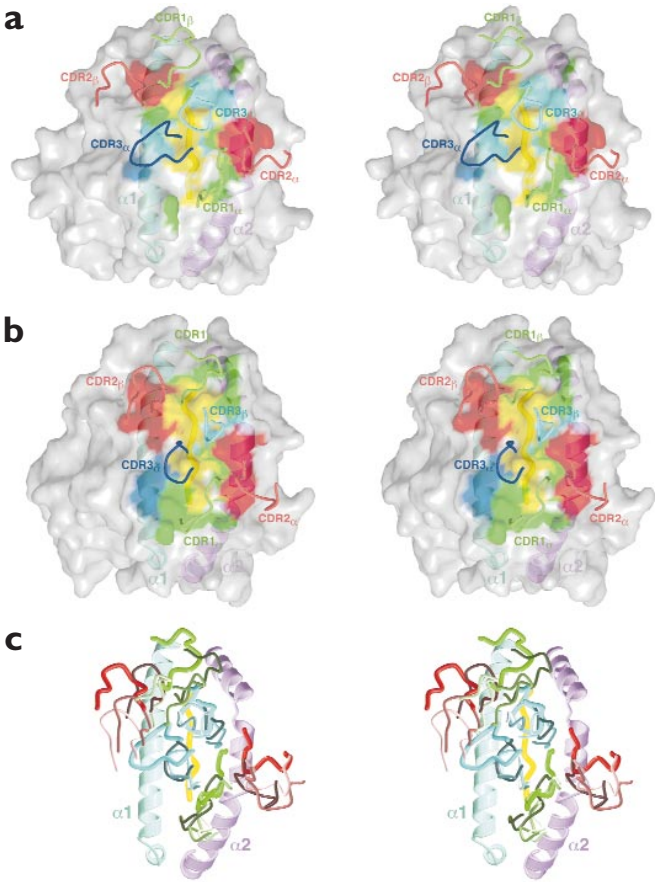

(this paper), it is tempting to speculate that peptide-specific alloreactive TCRs do contact the allo-MHC surface by a register similar to the one they used to contact the self-MHC molecules responsible for their selection. In that fixed docking frame, the allelic variability plausibly manifested by some of the residues available for TCR contact on the allogeneic MHC surface may accentuate their contribution to the overall binding energy (below).

Structures corresponding to the same TCR in complex with a self- and an allo-MHC are not available yet. Thus, to determine whether allorecognition is influenced by the selecting self-MHC molecule, we are left to analyze the partial sets of data obtained from the 2C and BM3.3 TCRs. Both self (dEV8–H-2K^b) and allogeneic (QL9–H-2L^d) ligands are known for the 2C TCR. In the 2C–dEV8–H-2K^b structure, the TCR contacts MHC α-helical residues that are mostly conserved between H-2K^b and H-2L^d, and the most parsimonious assumption is that it docks with a similar register on both self- and allo-MHC ligands[9].

Much less is known about the H-2^k–encoded ligand responsible for the intrathymic selection of the BM3.3 TCR and it remains to be determined whether it involves H-2D^k or H-2K^k molecules[20]. Reminiscent of the 2C TCR, the subset of H-2K^b residues contacted by the BM3.3 TCR is fully conserved in H-2D^k and shows a single mismatch at position 73 when compared to H-2K^k (serine in H-2K^b versus isoleucine in H-2K^k)[21]. In the BM3.3–pBM1–H-2K^b structure, the OG atom of Ser^{73} forms two hydrogen bonds with both the peptide and the TCR (**Fig. 2b** and **Table 1**). Although a serine to isoleucine substitution can be fit into the BM3.3–pBM1–H-2K^b structure without any steric clash, it will result in a precarious contact with the BM3.3 TCR.

Provided that H-2K^k controls the selection of the BM3.3 TCR, such an altered TCR-MHC contact should contribute to decrease the BM3.3–H-2K^k affinity within a range compatible with intrathymic selection, and to increase the relative energy contribution of foreign peptide residues recognized by the BM3.3 TCR in the context of self–H-2K^k molecules[8]. Alternatively, if H-2D^k controls the selection of the BM3.3 TCR, our results would indicate that H-2K^b and H-2D^k look the same in terms of the residues sensed by the BM3.3 TCR. Therefore, polymorphism limited to the residues lining the peptide-binding groove would allow a new repertoire of peptides to be seen, and thereby suffices to elicit high-affinity alloreactive T cells.

Whether the few peptide-independent alloreactive T cells that have been documented contrast with the peptide-specific ones and undergo a global repositioning upon binding to an allo-pMHC surface remains to be addressed at the structural level. Regardless of this plausible variation, our results are of interest for clinical applications[22,23] in that they provide a structural basis for the view that T cells specific for viral or tumor-associated peptides bound to allogeneic MHC molecules might have a higher precursor frequency and be easier to generate if the self-MHC molecules responsible for their selection and the MHC targets on allogeneic cells express a matched constellation of upward-pointing MHC α-helical residues. Conversely, selecting donor-recipient combinations that maximize the differences in the set of MHC residues sensed by the TCRs should be expected to dampen the strength of the T cell responses observed during allogeneic transplantation.

Methods

Protein expression. The BM3.3 T cell clone matured in a CBA/J background (H-2^k) and was isolated after immunization with the EL4 tumor cell line (H-2^b)[20,24]. The V module of the BM3.3 TCR was produced in myeloma cells as a single chain Fv fragment (scFV)[25], and the pBM1–H-2K^b binary complex was obtained by separately expressing the heavy chain of H-2K^b and β_2-microglobulin in bacteria. Each MHC subunit was purified as inclusion bodies and folded *in vitro* in the presence of the pBM1 peptide[26].

Identification of the endogeneous antigenic peptide recognized by the BM3.3 TCR. Peptide pBM1 was identified by microcapillary liquid chromatography and electrospray ionization mass spectroscopy from acid eluates of H-2K^b molecules immunopurified from the RMA lymphoma. pBM1 was the only candidate peptide that efficiently reconstituted the BM3.3 CTL epitope and co-eluted with endogeneous H-2K^b–binding peptides. pBM1 derives from a protein kinase related to the yeast protein SRP40 and is expressed at approximately 8,000 copies per cell (A. Guimezanes *et al*., unpublished data).

Biacore measurements. Measurements were carried out as described[27]. After purification on Superdex 200, 0.45, 0.9, 1.8, 3.6 and 7.2 μM of BM3.3 scFv TCR were injected at a flow rate of 5 μl per min over surfaces to which relevant (pBM1–H-2K^b, 2167RU) or irrelevant (pKB3–H-2K^b, 2286 RU) pMHC class I complexes had been immobilized. Both pMHC class I complexes were enzymatically biotinylated on the heavy chain COOH-terminus and size-purified on Superdex 200 before immobilization on streptavidin-coupled Research Grade CM5 Sensor chips (Biacore, Uppsala, Sweden).

Crystallography. Crystals were grown by the hanging drop method[28]. Crystals of the BM3.3–pBM1–H-2K^b complex were obtained from a solution in which the BM3.3 scFv TCR and the pBM1–H-2K^b binary complex were premixed for 24 h before crystallization assays at a 1:1 molar ratio and a final concentration of 4 mg/ml. The crystal used for the diffraction experiment ($200 \times 40 \times 10$ μm) was obtained at 4 °C in a drop formed by the addition of 2 μl of TCR-pMHC solution to 2 μl of crystallization solution (10% PEG 6000, 0.1 M HEPES pH 7.0, 0.25 M magnesium acetate, 0.25 M sodium chloride). The resulting crystal was transferred to a cryoprotectant solution identical to the crystallization solution except for the presence of 30% PEG 6000, and flashed-cooled at –160 °C under a nitrogen gas stream. The data set was collected at the European Synchrotron Radiation Facility, beamline D14eh3, using a 0.931 Å wavelength and a MAR-research CCD area detector. The crystal belongs to the $P2_12_12$ space group, with a = 76.6 Å, b = 120.4 Å, c = 102.9 Å, and contains one complex per asymmetric unit. Crystallographic data were processed with MOSFLM6.0[29] and SCALA of the CCP4 suite of programs[30]. The 99.9% complete data set extends up to 2.5 Å resolution with an R_{sym} of 0.084 and a redundancy of 7.2. The structure of the ternary complex was solved by the molecular replacement technique, using AmoRe[31] and the crystal structures of KB5-C20[32] and H-2K^b-OVA[33] as starting models. The final model was obtained after several rounds of manual building using O[34] and refinement using REFMAC[30] against data in the 12.0 to 2.5 Å resolution range. The final model includes 191 water molecules (12 water molecules form hydrogen bond bridges between BM3.3 TCR and pMHC) and has good refinement statistics (R_{free} = 0.276, R_{work} = 0.225, R_{cryst} = 0.221, r.m.s bond distance = 0.012 Å, r.m.s bond angle = 1.7°). The data collection and refinement statistics are shown in Web Table 2 on the supplmentary information page of *Nature Immunology* online. Accessible surface calculations were done with NACCESS[35] and Figures were generated with GRASP[36], MOLSCRIPT[37] and RENDER[38].

Functional studies using Ala-substituted pBM1 peptide variants. Spleen cells from BM3.3 TCR transgenic mice were stimulated with irradiated C57BL/6 spleen cells. After 3 d, cells were counted and their cytotoxic activity tested on ^{51}Cr-labeled RMA-S cells cultured at 26 °C for one night and pulsed for 1 h with various concentrations of wild-type pBM1 peptide or one of the singly alanine-substituted pBM1 variant peptides. Experiments were done at an effector to target ratio of 5:1 and used RMA-S target cells pulsed with a 10^{-7} M concentration of peptide.

Acknowledgements

We thank S. Nathenson for the pET-3a K^b and pET-3a B2m plasmids; P.A. van der Merwe for advice on surface plasmon resonance; P. Fourquet for peptide synthesis; J.Bonicel for mass spectrometry analysis; L. Leserman, J. Howard and P. Golstein for comments on the manuscript, W. Burmeister for help with synchrotron data collection at ESFR ID4eh3 beamline and N. Guglietta for editing the manuscript. T. M. was supported by a fellowship from ARC. This work was supported by institutional grants from CNRS, CEA, INSERM and a specific grant from ARC.

Coordinates of the BM3.3 TCR-pBM1/H2-K^b MHC complex have been deposited in the Protein Data Bank under accession number 1FO0.

Supplementary information is available on *Nature Immunology*'s website (http://immunol.nature.com) or as paper copy from the New York editorial office of *Nature Immunology*.

Received 10 July 2000; accepted 31 August 2000.

1. Goldrath, A.W. & Bevan, M. J. Selecting and maintaining a diverse T-cell repertoire. *Nature* **402,** 255–262 (1999).
2. Garcia, K. C. *et al.* Structural basis of plasticity in T cell receptor recognition of a self peptide-MHC antigen. *Science* **279,** 1166–1172 (1998).
3. Garboczi, D. N. *et al.* Structure of the complex between human T-cell receptor, viral peptide and HLA-A2. *Nature* **384,** 134–141 (1996).
4. Ding, Y. H. *et al.* Two human T cell receptors bind in a similar diagonal mode to the HLA-A2/Tax peptide complex using different TCR amino-acids. *Immunity* **8,** 1–20 (1998).
5. Lee, P. U.Y., Churchill, H. R. O., Daniels, M., Jameson, S. & Kranz, D. Role of the 2C T cell receptor residues in the binding of self- and allo-major histocompatibility complexes. *J. Exp. Med.* **191,** 1355–1364 (2000).

6. Rock E. P., Sibbald, P. R., Davis, M. M. & Chien, Y. CDR3 length in antigen-specific immune receptors. *J. Exp. Med.* **179,** 323–328 (1994).
7. Guimezanes, A., Schumacher, T. N. M., Ploegh, H. L. & Schmitt-Verhulst, A.-M. A viral peptide can mimic an endogeneous peptide for allorecognition of a major histocompatibility complex class I product. *Eur. J. Immunol.* **22,** 1651–1654 (1992).
8. Daniel, C., Horvath, S. & Allen, P. M. A basis for alloreactivity: MHC helical residues broaden peptide recognition by the TCR. *Immunity* **8,** 543–552.
9. Speir, J. A. *et al.* Structural basis of 2C TCR allorecognition of H-2L^d peptide complexes. *Immunity* **8,** 553–562 (1998).
10. Wang, J. *et al.* Atomic structure of an αβ T cell receptor (TCR) heterodimer in complex with an anti-TCR Fab fragment derived from a mitogenic antibody. *EMBO J.* **17,** 10–26 (1998).
11. Young, A. C., Zhang, W., Sacchettini, J. C. & Nathenson, S. G. The three-dimensional structure of H-2D^b at 2.4Å resolution: implications for antigen-determinant selection. *Cell* **76,** 39–50 (1994).
12. Braden, B. C., Goldman, E. R., Mariuzza, R. A. & Poljak, R. J. Anatomy of an antibody molecule: structure, kinetics, thermodynamics and mutational studies of the anti lysozyme antibody D1.3. *Immunol. Rev.* **163,** 45–57 (1998).
13. Zerrahn, J., Held, W. & Raulet, D. J. The MHC reactivity of the T cell repertoire prior to positive and negative selection. *Cell* **88,** 627–636 (1997).
14. Merkenschlager, M. *et al.* How many thymocytes audition for selection? *J. Exp. Med.* **186,** 1149–1158 (1997).
15. Jouvin-Marche, E. *et al.* Genomic organization of the mouse T cell receptor V$_\alpha$ family. *EMBO J.* **9,** 2141–2150 (1990).
16. Fremont, D. H., Matsumura, M., Stura, E. A., Peterson, P. A. & Wilson, I. A. Crystal structures of two viral peptides in complex with murine MHC class I H-2K^b. *Science* **257,** 919–927 (1992).
17. Malissen, M. *et al.* A T cell clone expresses two T cell receptor α genes but uses one αβ heterodimer for allorecognition and self MHC-restricted antigen recognition. *Cell* **55,** 49–59 (1988).
18. Bevan, M. J. High determinant density may explain the phenomenon of alloreactivity *Immunol. Today* **5,** 128–130 (1984).
19. Matzinger, P. & Bevan, M. J. Hypothesis: why do so many lymphocytes respond to major histocompatibility antigens? *Cell. Immunol.* **29,** 1–5 (1977).
20. Albert, F., Boyer, C., Buferne, M. & Schmitt-Verhulst, A.-M. Interaction between MHC-encoded products and cloned T cells. II. Analyses of physiological requirements indicate two different pathways of stimulation by class I alloantigens. *Immunogenetics* **19,** 279–294 (1984).
21. Pullen, J. K., Horton, R. M., Cai, Z. & Pease, L. R. Structural diversity of the classical H-2 genes: *K*, *D*, and *L*. *J. Immunol.* **148,** 953–967 (1992).
22. Little, M. T. & Storb, R. The future of allogeneic stem cell transplantation: minimizing pain, maximizing gain. *J. Clin. Invest.* **105,** 1679–1681 (2000).
23. Obst, R., Netuschil, N., Klopfer, K., Stevanovic, S. & Rammensee, H. G. The role of peptides in T cell alloreactivity is determined by self-major histocompatibility complex molecules. *J. Exp. Med.* **191,** 805–812 (2000).
24. Couez, D., Malissen M., Buferne, M., Schmitt-Verhulst, A. M. & Malissen, B. Each of the two productive T cell receptor α-gene rearrangements found in both the A10 and BM3-3 T cell clones give rise to an α chain which can contribute to the constitution of a surface-expressed αβ dimer. *Int. Immunol.* **3,** 719–729 (1991).
25. Grégoire, C., Malissen, B. & Mazza, G. Characterization of T cell receptor single-chain Fv fragments secreted by myeloma cells. *Eur. J. Immunol.* **26,** 2410–2416 (1996).
26. Zhang, W., Young, A. C. M., Imarai, M., Nathenson, S. G. & Sacchettini, J. C. Crystal structure of the major histocompatibility complex class I H-2Kb molecule containing a single viral peptide: implications for peptide binding and T-cell receptor recognition. *Proc. Natl Acad. Sci. USA* **89,** 8403–8407 (1992).
27. Willcox, B. E. *et al.* TCR binding to peptide-MHC stabilizes a flexible recognition interface. *Immunity* **10,** 357–365 (1999).
28. Wlodawer, A. & Hodgson, K. O. Crystallization and crystal data of monellin. *Proc. Natl Acad. Sci. USA* **72,** 398–399 (1975).
29. Leslie, A. G. W. in *Crystallographic Computing* (eds Moras, D., Podjarny, A. D. & Thierry, J. C.) 50–60 (Oxford Univ. Press, 1991).
30. Computational Project Number 4, CCP4, The CCP4 Suite: Programs for Protein Crystallography. *Acta Cryst.* **D50,** 760 (1994).
31. Navaza, J. AMoRe: an automated package for molecular replacement. *Acta Cryst.* **A50,** 157–163 (1994).
32. Housset D. *et al.* The three-dimensional structure of a T-cell antigen receptor V$_\alpha$V$_\beta$ heterodimer reveals a novel arrangement of the V$_\beta$ domain. *EMBO J.* **16,** 4205–4216 (1997).
33. Fremont, D. H., Stura, E. A., Matsumura, M., Peterson, P. A. & Wilson, I. A. Crystal structure of an H-2K^b-ovalbumin peptide complex reveals the interplay of primary and secondary anchor positions in the major histocompatibility complex binding groove. *Proc. Natl Acad. Sci. USA* **92,** 2479–2483 (1995).
34. Jones, T. A., Zou, J-Y., Cowan, S. W. & Kjeldgaard M. Improved methods for building protein models in electron density maps and the location of errors in these models. *Acta Cryst.* **A47,** 110–119 (1991).
35. Hubbard, S. J. & Thornton, J. P. "NACCESS" Computer Program, Department of Biochemistry and Molecular Biology, University College London (1993).
36. Nicholls, A., Scharp, K. A. & Honig, B. Protein folding and association: insights from the interfacial and thermodynamic properties of hydrocarbons. *Proteins Struct. Funct. Genet.* **11,** 281–296 (1991).
37. Kraulis, P. J. Molscript: a program to produce both detailed and schematic plots of protein structures. *J. Appl. Crystallogr.* **24,** 946–950 (1991).
38. Merrit, E. A. & Bacon, D. J. Raster 3D: photorealistic molecular graphics. *Meth. Enzymol.* **277,** 505–524 (1997).